Niobium Carbonitride Precipitation and Austenite Recrystallization in Hot-Rolled Microalloyed Steels

S. S. HANSEN, J. B. VANDER SANDE, AND MORRIS COHEN

The response of austenites to thermomechanical treatments is studied in a series of niobium (columbium) HSLA steels. Interactions between composition, plastic deformation, strain-induced precipitation, and austenite recrystallization are described and related to previous work in the field. Niobium in solution prior to deformation leads to significant retardation of subsequent austenite recrystallization if Nb(C,N) precipitation takes place prior to or during the early stages of recrystallization. Such strain-induced precipitation proceeds in two stages: initially at austenitic grain boundaries and deformation bands, and later on substructural features in the unrecrystallized austenite. The latter precipitation is accelerated only if it occurs in the unrecrystallized austenite; if recrystallization precedes Nb(C,N) precipitation, then the precipitation reaction is much slower. Thus, the Nb(C,N) precipitation and austenite recrystallization reactions are coupled phenomena. The conditions necessary for such an interaction are analyzed, and it is proposed that the level of supersaturation of Nb(C,N) in the austenite at the deformation temperature is a critical factor in determining whether or not an effective interaction will operate at that temperature.

HIGH-STRENGTH, low-alloy (HSLA) steels constitute a classical metallurgical development in which alloying additions and thermomechanical processing have been combined to attain desirable mechanical properties through microstructural control. Such process and compositional variations can develop yield strengths typically in the range of 350 t0 700 MPa (50 to 100 ksi), thus doubling the corresponding yield strength of mild steels. This increased strength, coupled with good toughness and weldability, has resulted in applications in transportation, pipeline, construction, and pressure-vessel technologies.

As presently available, HSLA steels are predominantly low in carbon (0.05 to 0.15 pct) and are alloyed with small quantities of strong carbide-forming elements such as niobium, vanadium or titanium.[1,2] This microalloying is intended to contribute to enhanced mechanical properties primarily through ferritic grain refinement, often supplemented by precipitation and/or substructural (dislocation) strengthening. Although recent comprehensive reviews dealing with the dependence of properties on the microstructure of microalloyed steels are available,[3-5] in the present context we need only highlight the following points. *Grain refinement* of the ferrite is the major mode of strengthening in HSLA steels. Based on a Hall-Petch type of strengthening increment,[6] a decrease of ferritic grain size from ASTM 6-8 (typical of hot-rolled mild steels) to ASTM 12-13 (typical of HSLA steels) is accompanied by an increase in yield strength of about 210 MPa (30 ksi). Concurrently, grain refinement is the only strengthening mechanism available in HSLA steels that simultaneously improves the toughness.[3] Thus, if other mechanisms are employed to raise the strength level, attaining the finest practicable ferritic grain size becomes even more important in order to compensate for the loss of toughness that would otherwise be introduced.

Such control of the ferritic grain size is in itself a complex subject, and has recently been considered elsewhere.[7] For our purposes, it can be stated that the finest ferritic grain sizes can be produced on transformation from austenite which remains unrecrystallized after hot rolling. Nb and other microalloying additions are known to retard austenite recrystallization, and this fact, together with the development of controlled rolling as a feasible commercial process,[8] has stimulated research aimed at defining the structural changes that occur in austenite during hot rolling.

Numerous investigators have studied the high-temperature deformation of austenite by means of hot compression,[9-13] hot tension,[14-16] hot torsion,[17,18] and hot rolling,[19-26] using a variety of techniques to monitor austenite recrystallization. These papers have generally shown a retarding effect of Nb on austenite recrystallization, and have variously ascribed this effect to "solute drag" or "precipitate pinning." However, relatively few workers have studied the concomitant niobium carbonitride [Nb,(C,N)] precipitation, or examined the potential interaction between this precipitation and the austenite recrystallization. Watanabe *et al*[27] used a wet chemical technique on electrolytically-extracted precipitates to follow quantitatively the Nb(C,N) precipitation reaction in unrecrystallized and recrystallized austenites. They found that the precipitation kinetics are about an order of magnitude faster in austenite that remains unrecrystallized after deformation. More recently, Weiss and Jonas[28,29] studied Nb(C,N) precipitation via hot compression testing,

S. S. HANSEN is an Engineer, Research Department, Bethlehem Steel Corporation, Bethlehem, PA 18016. J. B. VANDER SANDE and MORRIS COHEN are Associate Professor and Institute Professor Emeritus, respectively, Department of Materials Science and Engineering, Massachusetts Institute of Technology, Cambridge, MA 02139.

This paper is based on a presentation made at a symposium on "Precipitation Processes in Structural Steels" held at the annual meeting of the AIME, Denver, Colorado, February 27 to 28, 1978, under the sponsorship of the Ferrous Metallurgy Committee of The Metallurgical Society of AIME.

ISSN 0360-2133/80/0311-0387$00.75/0

utilizing changes in the strain-to-peak stress (*i.e.*, the strain required to initiate dynamic recrystallization) to follow the reaction. They also observed accelerated precipitation kinetics in deformed austenites, up to two orders of magnitude faster when the precipitation occurs dynamically.

LeBon *et al*[18] used hot-torsion testing, determining the austenite recrystallization metallographically, and attempting to follow the Nb(C,N) precipitation reaction via microhardness measurements on samples quenched after testing. Although the hardness testing proved to be rather unreliable for defining the precipitation kinetics, their recrystallization data included two significant effects. A peculiar recrystallization/time/temperature (*RTT*) curve was generated for the 0.04 pct Nb steel studied, in that *C*-curve recrystallization kinetics were observed below 950°C. While a slight retarding effect of Nb above 950°C was ascribed to solute drag, the *C*-curve kinetics below 950°C were attributed to an interaction between recrystallization and strain-induced Nb(C,N) precipitation, an idea which was later amplified by Weiss and Jonas.[28,29] Furthermore, LeBon *et al*[18] clearly showed that Nb in solution prior to deformation is necessary for recrystallization retardation, inasmuch as 4 to 5 nm precipitates existing *prior* to deformation had no effect on the austenite recrystallization. More recently, Hoogendoorn *et al*,[25] using single-pass rolling, found a pronounced retardation of austenite recrystallization below 950°C. However, their *RTT* diagram disclosed no *C*-curve kinetics, the rate of recrystallization decreasing monotonically with decreasing temperature. Their Nb(C,N) precipitation kinetics (followed by X-ray fluorescence of extracted precipitates) were appreciably slower than reported by Watanabe *et al*,[27] and there was no apparent interaction between the austenite recrystallization and the Nb(C,N) precipitation.

The most recent work in this area by Davenport *et al*[26] has indicated no recrystallization in a 0.09 pct Nb steel, deformed by single-pass rolling, at temperatures below 1000°C. At the same time, the Nb(C,N) precipitation reaction was followed semi-quantitatively by X-ray diffraction of extracted precipitates and *C*-curve kinetics were found, the nose of the *C*-curve lying above 980°C. With dark-field transmission electron microscopy, Nb(C,N) precipitates were detected on what appeared to be prior austenitic subboundaries, in agreement with previous researchers[20] who had used this evidence to suggest that precipitate pinning is the operative mechanism in retarding austenite recrystallization.

The results of the foregoing papers may be summarized as follows:

1. Niobium in solid solution prior to deformation can lead to a marked retardation of austenite recrystallization, especially in the lower temperature range of the austenitic phase field. This effect of niobium is lost, however, if the niobium is precipitated as Nb(C,N) *prior* to deformation.
2. When niobium acts to substantially retard austenite recrystallization, strain-induced precipitation of Nb(C,N) is typically observed.
3. The data suggest that the retarding effect of niobium on austenite recrystallization is due to a solute-drag or precipitate-pinning mechanism, but unequivocal evidence for one or the other is still lacking.

The present investigation is aimed at providing further information on how the hot deformation of austenite affects Nb(C, N) precipitation and how the latter, in turn, influences the recrystallization process in HSLA steels. In other words, we are specifically concerned here with the nature of the interaction between strain-induced precipitation and austenite recrystallization.

EXPERIMENTAL PROCEDURE

Processing of Steels

This investigation focussed on five steels, whose compositions are shown in Table I, all prepared as electric-furnace-melted 500-pound ingots.

The base composition (steel 1) was a low-carbon, aluminum-killed steel containing 1.3 pct Mn. To this base, increasing additions of niobium were made as follows: (i) 0.03 pct—a typical commercial niobium addition; (ii) 0.095 pct—based on published solubility data,[30] this represents the maximum amount of niobium that should be soluble at 1250°C in a 0.1 pct C, 0.01 pct N austenite; and (iii) 0.21 pct—here, at least half of the niobium should remain undissolved at 1250°C.

Additionally, the effect of manganese as a compositional variable was investigated at the 0.03 pct Nb level (steels 2 *vs* 5).

These steels were all laboratory hot-rolled on a four-high reversing mill* to 12.5 mm (1/2 in.)-thick plate, and air-cooled. For subsequent rolling experiments, small specimens (37.5 mm × 18.75 mm × 12.5 mm) were cut from these plates, preserving the original rolling direction, and sheathed thermocouples were inserted at mid-thickness, about 12.5 mm in from the rear of the sample.

*The material used in this investigation was supplied by Bethlehem Steel Corporation, and was made and processed at the Homer Research Laboratories

The hot-rolling schedule adopted for this study is illustrated in Fig. 1. All the specimens were initially soaked for one hour to dissolve all or a portion of the Nb(C,N) precipitates. Most experiments involved a solutionizing temperature of 1250°C, although in one case, steel 2 was also soaked at 1100°C. The specimens were then transferred to a salt pot maintained at 950°C in order to bring the steel to the selected rolling temperature. Five minutes in this pre-rolling salt pot was chosen as a convenient time for thermal equilibration, and should involve minimal Nb(C,N) precipitation in the undeformed austenite.[27]

Table I. Compositions of Steels (Wt Pct)

Steel No	C	Mn	Si	P	S	Nb	Al	N
1	0.11	1.30	0.25	0.009	0.003	<0.005	0.017	0.0085
2	0.11	1.35	0.26	0.008	0.004	0 031	0.023	0.010
3	0.10	1.24	0.23	0.010	0.004	0.095	0.014	0.010
4	0.10	1.32	0.25	0.009	0.003	0.21	<0.010	0.010
5	0.11	1.99	0.23	0.007	0.004	0.029	0.026	0.010

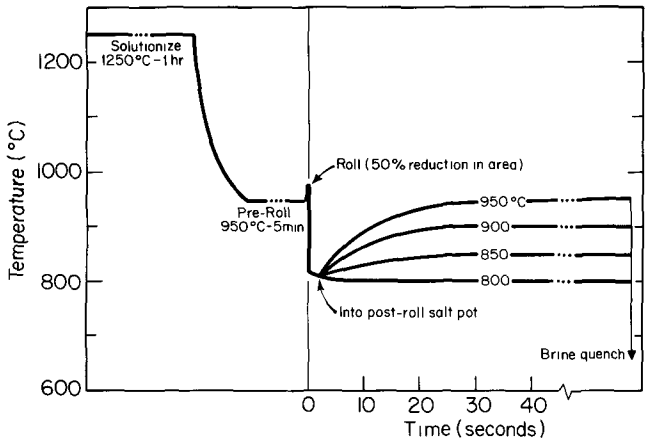

Fig. 1—Temperature/time cycle for thermomechanical treatments employed in hot-rolling experiments.

The specimens were then rolled in a single pass to a 50 pct reduction using a two-high 381 mm (15 in.) diameter laboratory rolling mill;* this step caused a temperature drop of about 130°C after some prior adiabatic heating, as registered by the inserted thermocouple. The deformed samples were then transferred to a post-rolling salt pot which was maintained at temperatures from 800 to 950°C; thermal equilibration times ranged from 5 s at 800°C to 30 s at 900 and 950°C. The samples were held in this salt pot for times up to 10,000 s, followed by quenching in a 6 pct brine solution at 20°C. After such treatments, the specimens were cut-up for metallographic examination at the middle third of the rolled section.

*Assuming sticking friction,[31] the mean strain rate was calculated to be about 2.6/s.

Recrystallization Measurements

The austenite recrystallization was measured metallographically by point counting on a longitudinal section (containing the rolling direction and the rolling-plane normal) of the brine-quenched specimens, with the prior austenitic structure delineated in the martensitic matrix in the following ways. For steels 2 to 4, a small amount of ferrite formed at the prior austenitic boundaries, even on brine quenching, and 1 pct nital for 4 to 5 s then worked quite well as the etchant. However, in steels 1 and 5, no ferrite was detected on quenching, and a hot etch (50 to 60°C) for 5 to 7 min in a solution of saturated aqueous picric acid plus 2 vol pct of Trenamine W-35* was successful in bringing out the prior austenitic boundaries. The latter etch produces a black surface film which is then removed by swabbing in denatured alcohol. This etching procedure was satisfactory for all samples studied here, producing results equivalent to nital in steels 2 to 4. However, because of the comparative ease of etching with nital, the hot picric acid was only used when necessary.

*Trenamine W-35 is supplied by the Alco Chemical Corporation, Philadelphia, PA. This is a commercial wetting agent, sodium alkyl sulfonate, and is similar to the "Teepol" suggested in other investigations.[18]

Nb(C,N) Precipitation Measurements

The precipitation of Nb(C,N) in the above samples was monitored via particle-size distribution and particle area-density measurements made on direct carbon extraction replicas, employing an analysis due to Ashby and Ebeling.[32] In this method, the polished specimens are first etched with 1 pct nital for about 3 s and then a thin layer of carbon is evaporated onto the etched surface, after which the samples are immersed in 10 pct nital for up to 2 min. The carbon film is next floated off by immersion in distilled water, collected on a copper grid, and examined by electron microscopy. The relevant measurements were made on micrographs taken from different areas of several replicas for each of the samples studied.

RESULTS

Structures Prior to Deformation

Since both the austenite recrystallization, and the Nb(C,N) precipitation may be influenced by the austenitic grain size, and the amount of niobium in or out of solution, the microstructures existing prior to rolling were investigated by brine quenching directly from the pre-roll salt pot. As shown in Table II, the plain-carbon and 0.03 pct Nb steels are relatively coarse-grained after solutionizing at 1250°C, while the higher-niobium steels are progressively finer grained. The finest austenitic grain size, however, is produced in steel 2 (0.03 pct Nb), after soaking at 1100°C (~ASTM6). Examination of carbon extraction replicas revealed that no fine precipitates (< 10 nm in size) are present prior to rolling, and it is therefore concluded that all of the niobium dissolved at the solutionizing temperature remains in solution during the pre-roll equilibration period. On the other hand, coarse undissolved precipitates are found in the higher-niobium steels (3 and 4), and in steel 2 after solutionizing at 1100°C (Fig. 2). These undissolved carbonitrides inhibit grain coarsening at the solutionizing temperature, as proposed by Zener[33] and Gladman.[34] In fact, Gladman's precipitate-pinning model is in relatively good quantitative agreement with these experimental observations.

The presence of undissolved carbonitrides in steel 3 (0.095 pct Nb) following a 1250°C solutionizing treatment is not consistent with Nordberg and Aronsson's solubility equation[30] which predicts complete solution of this niobium content at this temperature. Thus, for purposes of calculation, the solubility equation of Irvine *et al*[2] has been adopted here. Assuming a stoichiometric precipitate, $Nb(C_xN_{1-x})$ and

Table II. Austenitic Grain Sizes and Dissolved Niobium Prior to Rolling

Steel	Solutionizing Temperature, °C	Austenitic Grain Size, μm	Precipitate Size, μm	Niobium in Solution, Pct*
1 (nil Nb)	1250	325	–	nil
2 (0.031 Nb)	1250	405	–	0.031
	1100	40	0.04 to 0.1	0.018
3 (0.095 Nb)	1250	140	0.2 to 0.4	0.069
4 (0.21 Nb)	1250	55	0.2 to 0.4	0.072
5 (0.029 Nb) (1.99 Mn)	1250	490	–	0.029

*These levels of dissolved niobium are based on the solubility equation proposed by Irvine *et al.*[2]

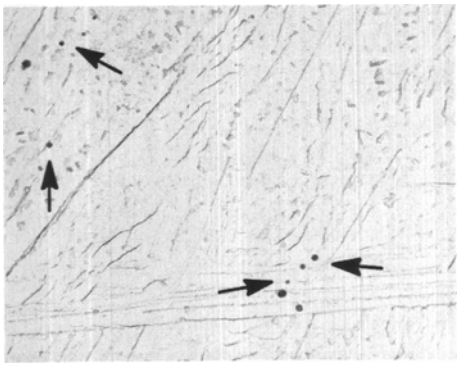

(a)

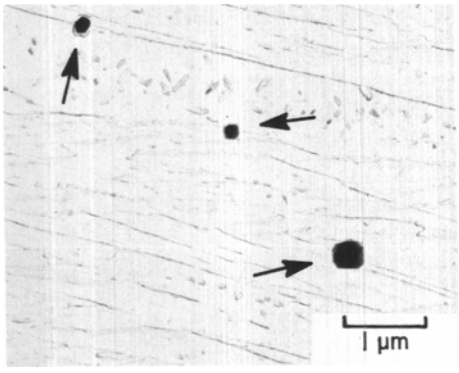

(b)

Fig. 2—Carbon extraction replicas illustrating the undissolved Nb(C, N) phase (discrete black particles indicated by arrows) present prior to rolling. (*a*) Steel 2, solutionized at 1100°C. (*b*) Steel 4, solutionized at 1250°C. The samples were solutionized for 1 h, then held at 950°C for 5 min and brine quenched.

considering the nitrogen as an equivalent atom proportion of carbon, their equation can be written as:

$$\log_{10}\left([\text{pct Nb}] \cdot \left[\text{pct C} + \frac{12}{14}\text{pct N}\right]\right) = 2.26 - \frac{6770}{T(\text{K})}.$$

The resulting level of niobium soluble in each of the steels after solutionizing is shown in Table II. This dissolved niobium turns out to be an important parameter in affecting the response of these steels to thermomechanical processing, but the variation in austenitic grain size and in the density of undissolved carbonitrides should also be considered.

Microstructural Aspects of Austenite Recrystallization

The microstructural changes occurring during rolling were evaluated in samples quenched directly off the rolls. A typical deformed structure is shown in Fig. 3. In addition to the pancaking of the austenitic grains, the rolling process produces a substantial number of deformation bands in the as-rolled microstructure. These deformation bands are not uniformly distributed, thereby demonstrating the heterogeneous nature of the plastic deformation in rolling.

The initial stage of austenite recrystallization appears to be highly localized (Fig. 4), but not the early site saturation that has been observed for other hot-worked structures.[35] Recrystallized grains nucleate predominantly at austenitic grain boundaries, and are frequently observed at the intersection of three grains (Fig. 4(*a*) and (*b*)). Deformation bands, deformed twin boundaries, and inclusions may also provide effective nucleation sites. Although most of the recrystallization centers are observed only after some degree of growth, occasional highly-serrated austenitic boundaries are found (Fig. 4(*c*)), which may signal the start-up of recrystallization at those places.

The progress of recrystallization is illustrated in Fig. 5 for steel 3 (0.095 pct Nb). The start-up of recrystallization is highly nonuniform, and even as the reaction proceeds, many of the prior austenitic boundaries remain unactivated as nucleation sites. The unrecrystallized areas are progressively consumed as the recrystallization front migrates into the unrecrystallized regions. Relatively rapid recrystallization kinetics are observed at 950°C; after 10,000 s, the reaction is virtually complete. Slower rates are evident at lower temperatures, and in fact, at 800°C, ferrite nucleation precedes any detectable recrystallization in all the steels except for the nil-niobium steel.

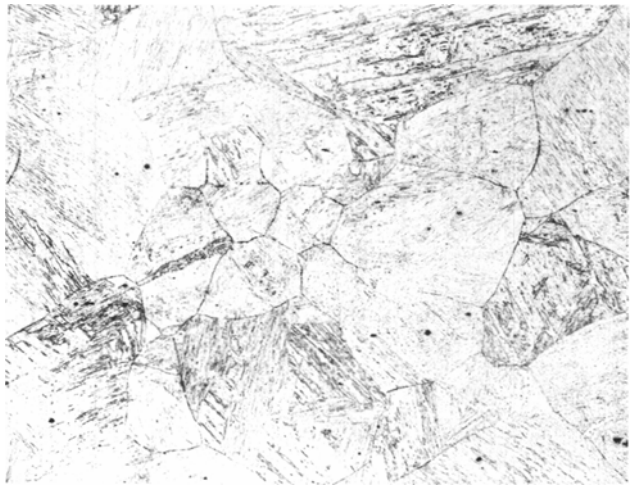

(a)

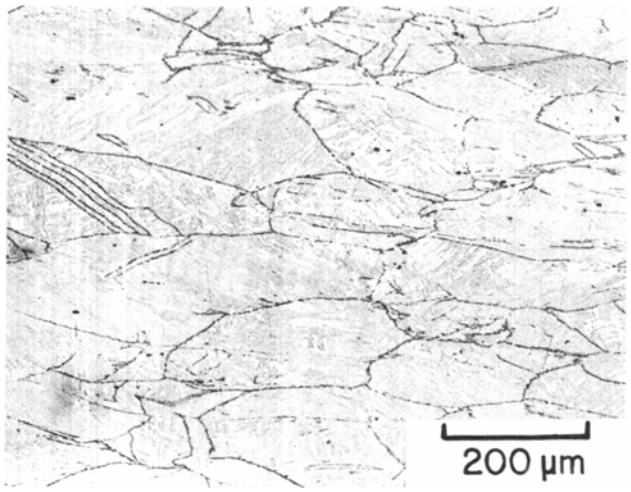

(b)

Fig. 3—Micrographs of steel 3 showing structure (*a*) prior to rolling (1250°C—1 h, 950°C—5 min), and (*b*) after hot rolling 50 pct at 950°C.

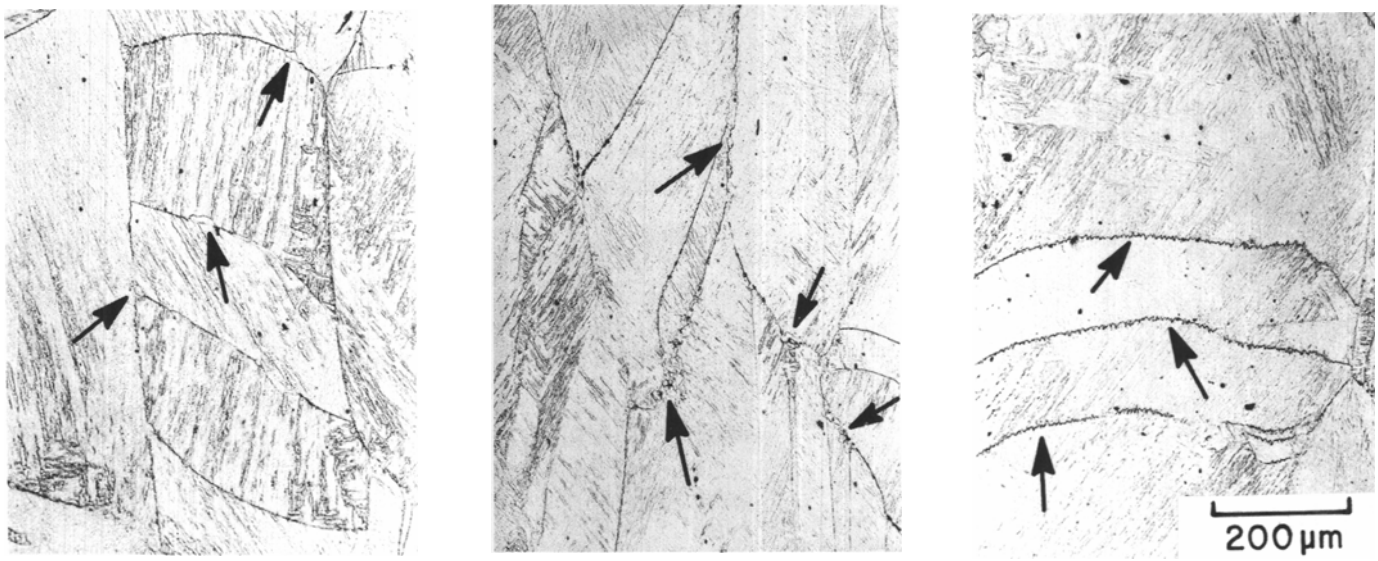

Fig. 4—Micrographs of steel 5 illustrating the initial stages of recrystallization (arrows) observed after hot rolling 50 pct at 950°C and holding at 850°C for 10,000 s.

Isothermal Recrystallization Kinetics

The volume fraction of austenite recrystallized is plotted against time in Figs. 6 through 8 for all steels held at post-rolling temperatures from 850 to 950°C. The curves shown are not corrected for the heating times required to attain a given holding temperature. Although such a correction could be made from a knowledge of the appropriate heating curve and the activation energy for recrystallization, using the method proposed by Wells,[36] it is dubious if a meaningful activation energy could be determined for these steels inasmuch as the mechanisms of recrystallization, and hence the rate-controlling steps, vary with temperature. Accordingly, the present data are simply plotted against time in the post-roll salt pot, noting that the thermal equilibration times were about 20 s at 850°C and about 30 s at 900 and 950°C.

The steels investigated here are usually unrecrystallized in quenching off the rolls (*i.e.*, within 2 s after rolling); exceptions are the Nb-free steel, and steel 2 solutionized at 1100°C. In these instances, recrystallization either begins during rolling (dynamic recrystallization) or with a negligible incubation time after rolling (rapid static recrystallization). Considering the recrystallization/time curves, it is obvious that niobium retards the austenite recrystallization kinetics at all the post-rolling temperatures employed. However, the use of a lower soaking temperature, and thus a reduced level of dissolved niobium prior to rolling, in steel 2 drastically increases the recrystallization kinetics at 950°C, although the rate is still slower than that of the Nb-free steel.* These results suggest that the amount of niobium in solution in this steel prior to rolling is below a critical level necessary for major recrystallization retardation at 950°C. Apparently, 0.03 pct Nb in solution is effective in this respect, whereas 0.018 pct Nb is not.

All the niobium steels solutionized at 1250°C behave consistently at all post-rolling temperatures; the recrystallization reaction is retarded significantly by the niobium, and is virtually eliminated at 850°C. At higher holding temperatures, the kinetics are faster, but only at 950°C does significant recrystallization occur within the time frame considered here. Among these niobium steels, steel 4 (0.21 pct Nb) displays the fastest recrystallization kinetics (but also had the finest austenitic grain size prior to rolling), while steel 3 (0.095 pct Nb) exhibits the slowest kinetics. No significant effect of manganese is found at the two alloying levels; indeed, the recrystallization kinetics of steels 2 and 5 are similar at all the post-rolling temperatures studied.

As detailed previously, the austenitic grain size and the density of undissolved carbonitrides varies from steel-to-steel. While these undissolved carbonitrides appear too coarse to retard recrystallization at the post-rolling temperatures, the particles may have acted to accelerate recrystallization by providing heterogeneous nucleation sites.[37]

The effect of austenitic grain size on the post-rolling recrystallization kinetics is also difficult to rationalize, but an attempt can be made towards separating the factors due to grain size, dissolved niobium, and undissolved carbonitrides by assuming that the time for 50 pct recrystallization is proportional to the austenitic grain diameter prior to rolling. Cahn[38] has derived such a relationship under conditions of grain-boundary nucleation, site saturation, and a constant growth rate—conditions which are not fulfilled in these experiments. While recognizing these limitations, we have adopted the above assumptions in order to ascribe some order of magnitude to the various possible contributions. On this basis, calculated values (f_{gs}) are given in Table III, indicating the factors by which the time to 50 pct recrystallization would change if "normalized" to the grain size of

*In a related experiment which will be reported elsewhere, a 0.02 pct Nb semi-killed steel exhibited similar recrystallization kinetics to steel 2 (1100°C solutionizing temperature) at 950°C. On holding this semi-killed steel at lower post-rolling temperatures, however, the recrystallization rate was progressively retarded, such that at 850°C the recrystallization rate was about three orders of magnitude slower than in the Nb-free steel.

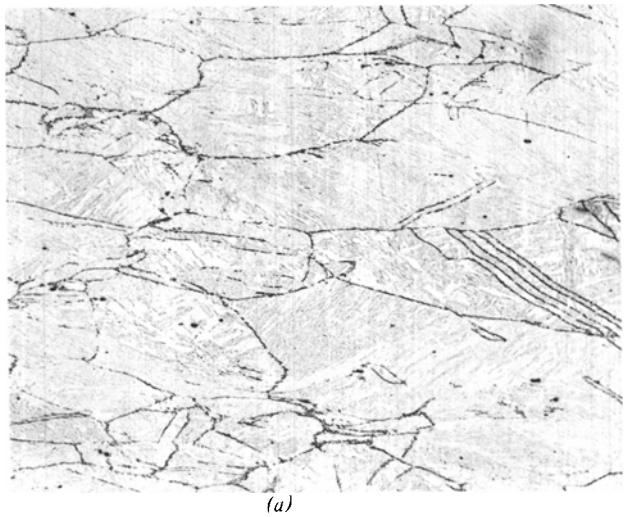

(a)

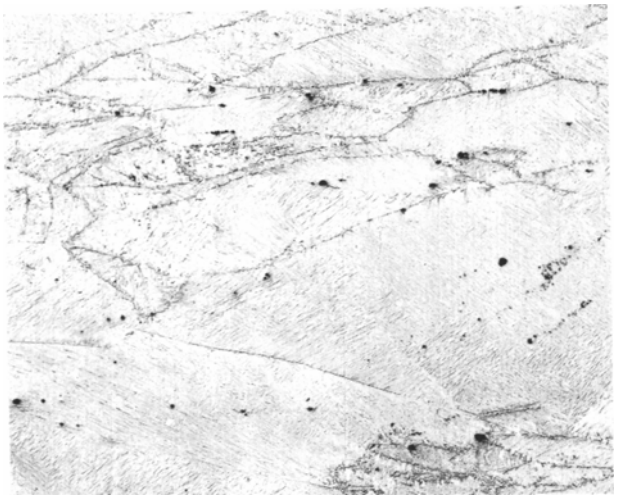

(b)

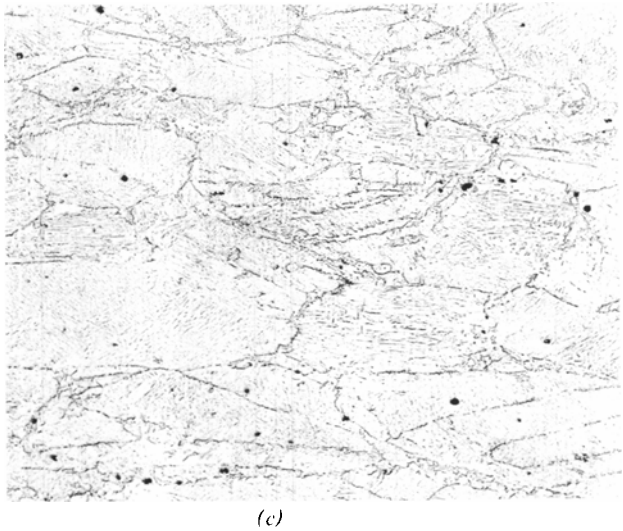

(c)

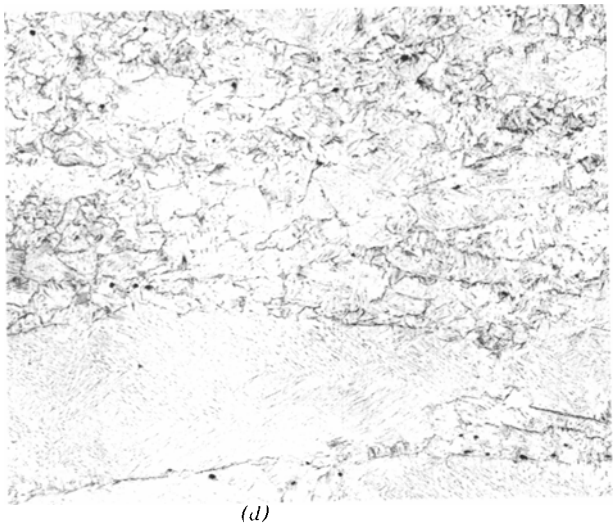

(d)

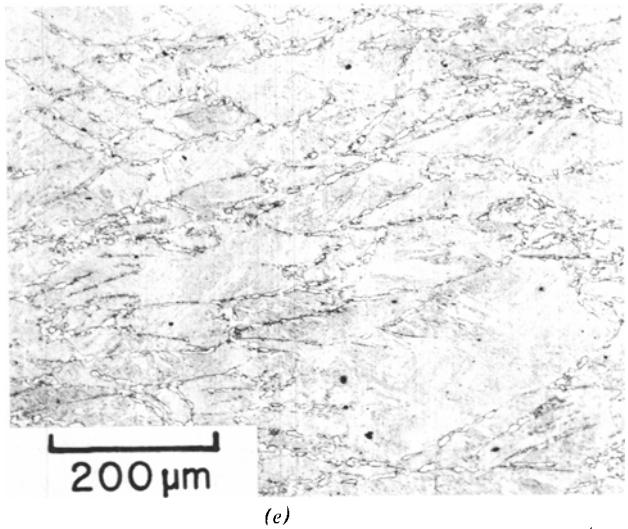

(e)

Fig. 5—Progress of recrystallization in steel 3 following 50 pct reduction by hot rolling at 950°C. (*a*) As-rolled. (*b*) Rolled and held at 950°C for 100 s. (*c*) Rolled and held at 950°C for 1,000 s. (*d*) Rolled and held at 950°C for 10,000 s. (*e*) Rolled and held at 800°C for 10,000 s. (Note: At 800°C, ferrite nucleation precedes austenite recrystallization).

steel 1. Similarly, based on the recrystallization/time curves, and ignoring the aforementioned thermal-equilibration times, the observed 50 pct recrystallization times can be compared by ratio (f_{obs}) with the 50 pct recrystallization time for the Nb-free steel. Then, in a very approximate way, the effect of niobium as a compositional variable (f_{Nb}) in these steels can be obtained by taking $f_{Nb} = f_{obs}/f_{gs}$. The values thus determined are listed in Table III, and indicate that the recrystallization kinetics are retarded substantially by the amount of niobium dissolved in the austenite prior to rolling. In contrast, the undissolved carbonitrides (0.2 to 0.4 μm in size) do not appear to affect the recrystallization kinetics significantly, considering that the f_{Nb} factors for steels 3 and 4 are rather similar.

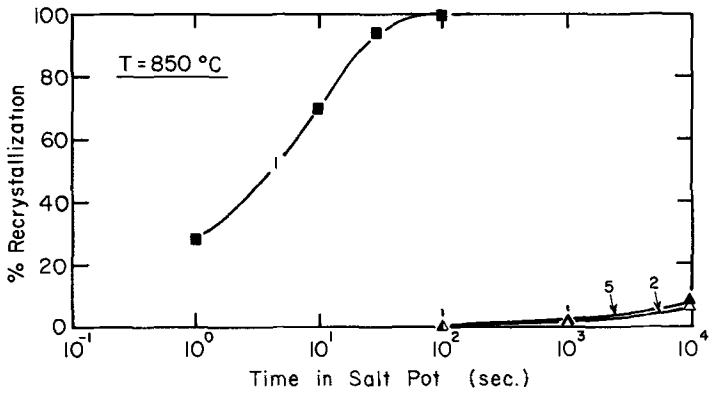

Fig. 6—Course of austenite recrystallization at 850°C after hot rolling 50 pct at 950°C.

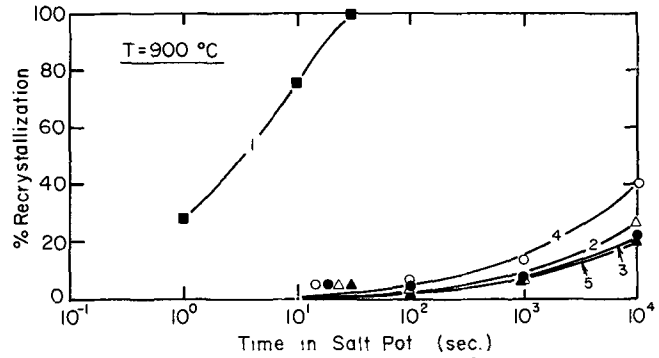

Fig. 7—Course of austenite recrystallization at 900°C after hot rolling 50 pct at 950°C.

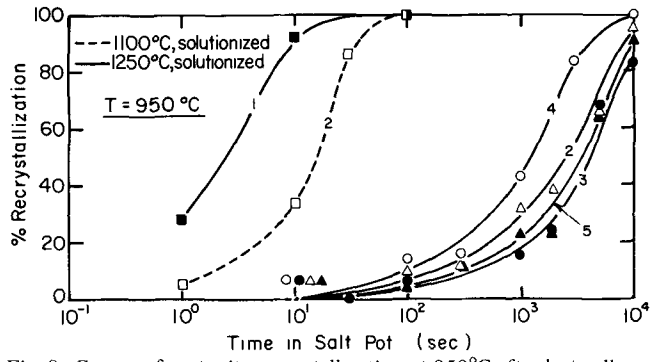

Fig. 8—Course of austenite recrystallization at 950°C after hot rolling 50 pct at 950°C.

Recrystallization-Front Growth Rates

Cahn and Hagel[39] have shown that the rate of a transformation can be described by an expression of the form, $dx/dt = GS_v$, where dx/dt is the rate of transformation on a volume basis, **G** is the average migration rate of moving boundaries, and S_v is the interfacial area (per unit vol) between the transformed and untransformed regions. This relationship has been applied previously in studies of recrystallization,[35,40] and was employed in this investigation to determine the migration rates of the recrystallization fronts, particularly in steels where the recrystallization behavior differed markedly. In this connection, the results for steel 2 (solutionized at 1100 and 1250°C) and steel 3 are presented to illustrate how the recrystallization growth rate (at 950°C) varies with the amount of niobium in solid solution prior to rolling. As shown in Fig. 9, **G** is found to decrease rapidly during the initial stages of recrystallization, and then less so as the recrystallization proceeds. In addition to these trends, the rates also decrease with increasing niobium in solid solution prior to rolling. The difference in effect between 0.018 and 0.03 pct Nb in solution is especially noteworthy.

Precipitation Processes in Hot-Rolled Austenites

The precipitation reactions occurring in these steels on holding in the austenitic range subsequent to hot rolling were studied by transmission electron microscopy of carbon extraction replicas. Precipitate-size distributions and area densities were determined by this technique. Particles smaller than about 2 nm in size could not be detected on the replicas, and hence are missing from the volume fractions to be discussed.

On the assumption of spherical particles as extracted by the replicas, the precipitate volume fraction, f, is given by:[32]

$$f = \frac{\pi}{6}\left[\frac{N'_S}{\alpha}(x_A^2 + \sigma_A^2)\right]$$

where,

Table III. Calculated Factors for Niobium Effect in Retarding Austenite Recrystallization at 950°C

Steel	Solutionizing Temperature, °C	Niobium in Solution, Wt Pct	Austenitic Grain Size, μm	Austenitic Grain $[f_{gs}]$	50 Pct Recrystallization Time, s	50 Pct Recrystallization $[f_{obs}]$	f_{Nb}*
1	1250	nil	325	[1]	2.5	[1]	–
2	1250	0.031	405	[1.25]	2750	[1100]	880
	1100	~0.018	40	[0 12]	15	[6]	50
3	1250	0.069	140	[0.43]	4000	[1600]	3720
4	1250	0.072	55	[0.17]	1350	[540]	3180
5	1250	0.029	490	[1.5]	3250	[1300]	870

*$f_{Nb} = f_{obs}/f_{gs}$.

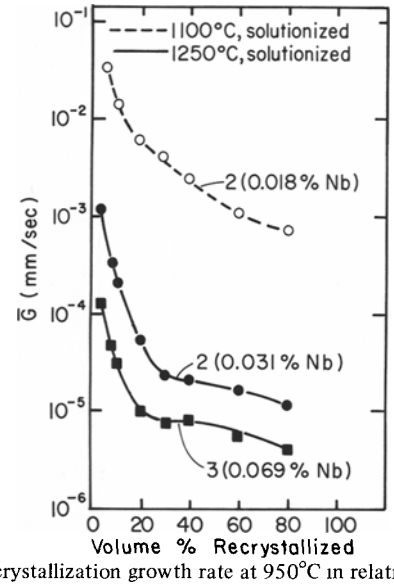

Fig. 9—Recrystallization growth rate at 950°C in relation to volume fraction recrystallized and amount of niobium dissolved in austenite prior to 50 pct hot rolling at 950°C.

N'_S = measured number of particles per unit area on the extraction replica,

α = extraction efficiency; here the surface depth replicated is taken as $2x_A$, and the extraction efficiency thus incorporates this variable,

x_A = arithmetic mean of particle diam,

σ_A = standard deviation from this mean.

Ashby and Ebeling[32] showed that, although the particle-size distribution is independent of the extraction efficiency, the volume fraction clearly is not. Thus, the technique was judged to be unsuitable for determining the volume fraction of precipitates, especially very fine precipitates, with any reasonable degree of accuracy. However, if a parameter (K) is defined such that $K = N'_S(x_A^2 + \sigma_A^2) = 6\alpha f/\pi$, and if α is taken to be roughly constant for the standardized replicating technique adopted in this study, then K becomes proportional to the precipitate volume fraction and can be used to follow the *changes* in the precipitate volume fraction, at least in a semi-quantitative manner.

The precipitation reactions in these steels are found to be essentially of two types. In the Nb-free steel, precipitates are observed only after long holding times, well after the austenite recrystallization is complete. These precipitates are all fairly coarse and relatively sparse (Fig. 10), and occur primarily at prior austenitic grain boundaries. Analysis of these precipitates in a scanning transmission electron microscope (STEM) shows them to be aluminum-rich and are thus believed to be aluminum nitrides. In the niobium steels, there is an initial rapid precipitation at prior austenitic grain boundaries and deformation bands after rolling (Fig. 11(*a*)), and the particles coarsen quickly on further holding. Later, a more general precipitation sets in, mainly on prior austenitic subboundaries (Fig. 11(*b*)) in the unrecrystallized austenite, in agreement with previous findings.[20,26] These precipitates were identified by energy-dispersive analysis in a STEM as niobium-rich, and are thus taken to be Nb(C,N). The rate of this matrix precipitation, as followed by measurements of the K parameter on extraction replicas, is found to depend on the temperature and the degree of supersaturation, being faster at higher temperatures and with larger amounts of niobium in supersaturated

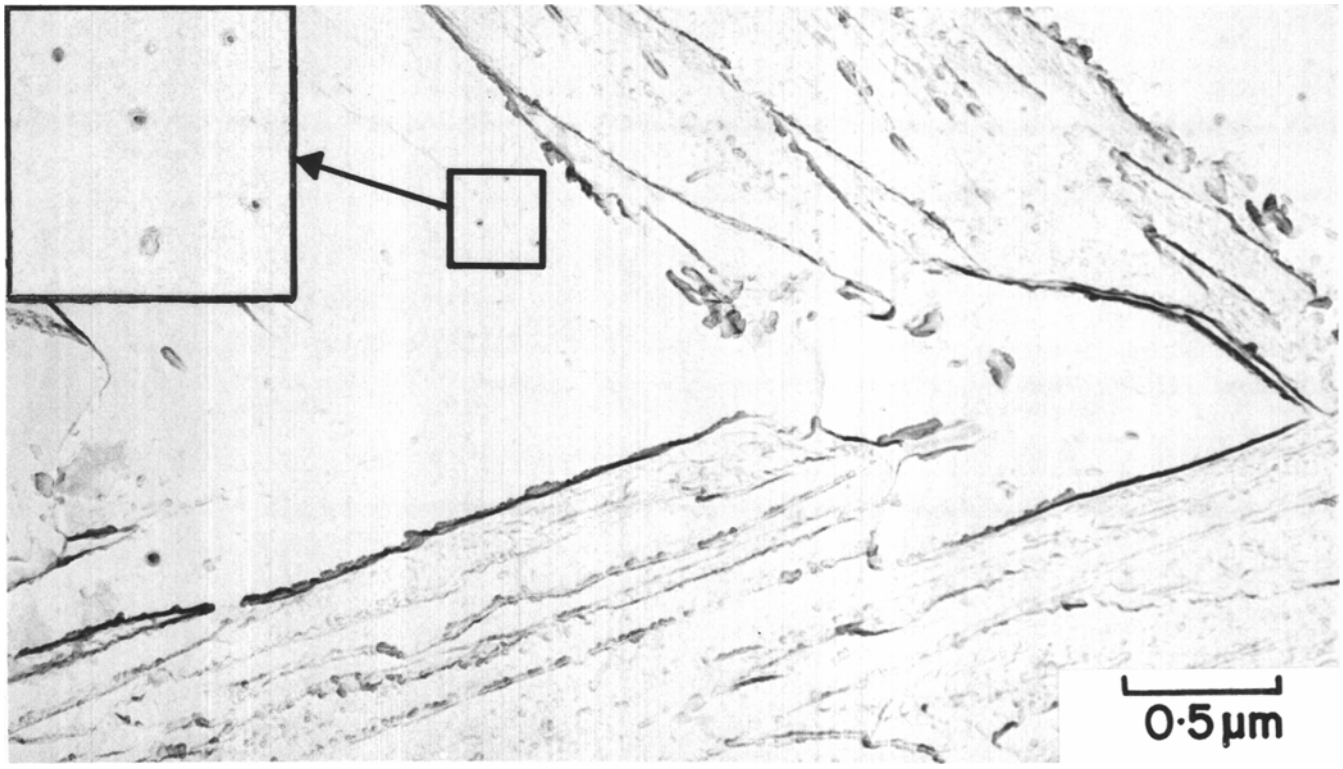

Fig. 10—Carbon extraction replica of aluminum nitride precipitates in the niobium-free steel 1 after hot rolling 50 pct at 950°C and holding at 900°C for 10,000 s. Insert shows fine AlN particles at a further magnification of 2.5 times.

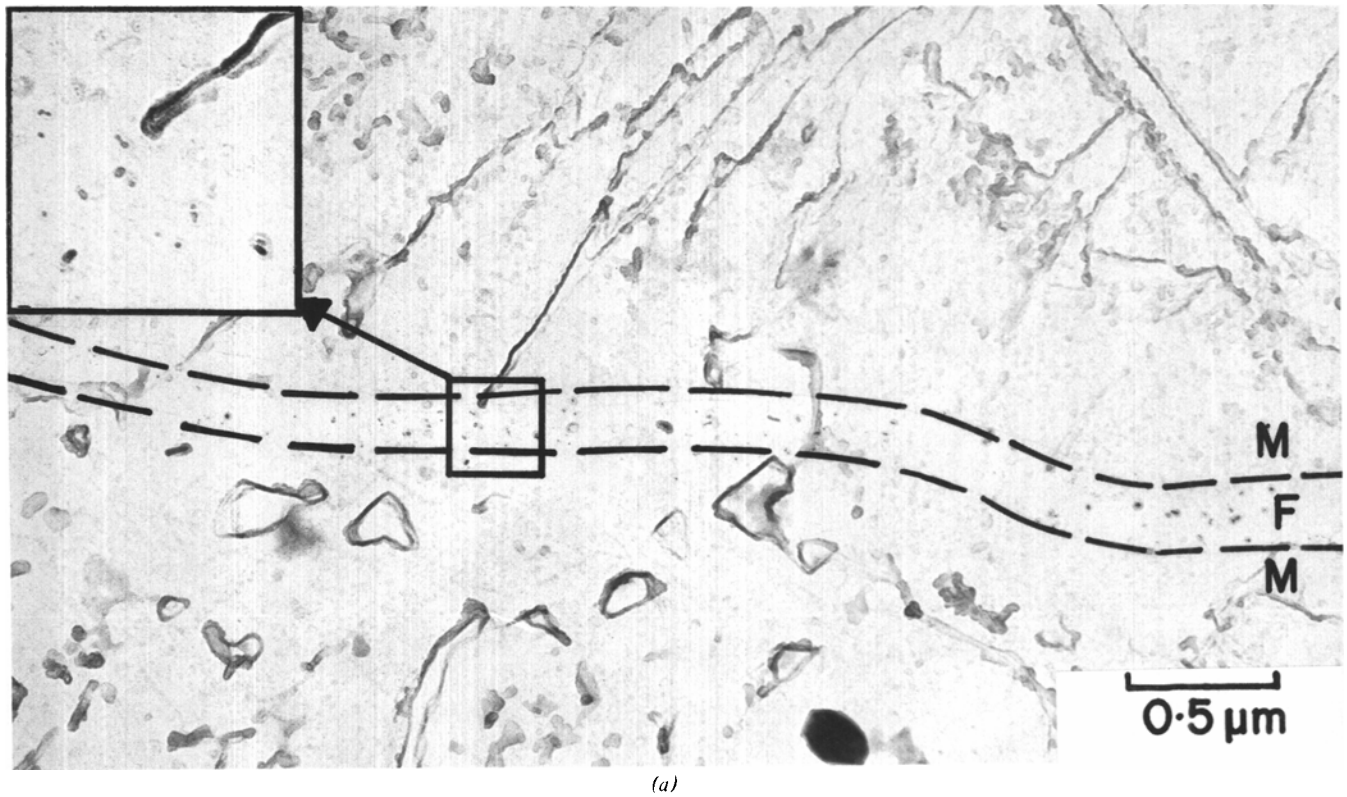

(a)

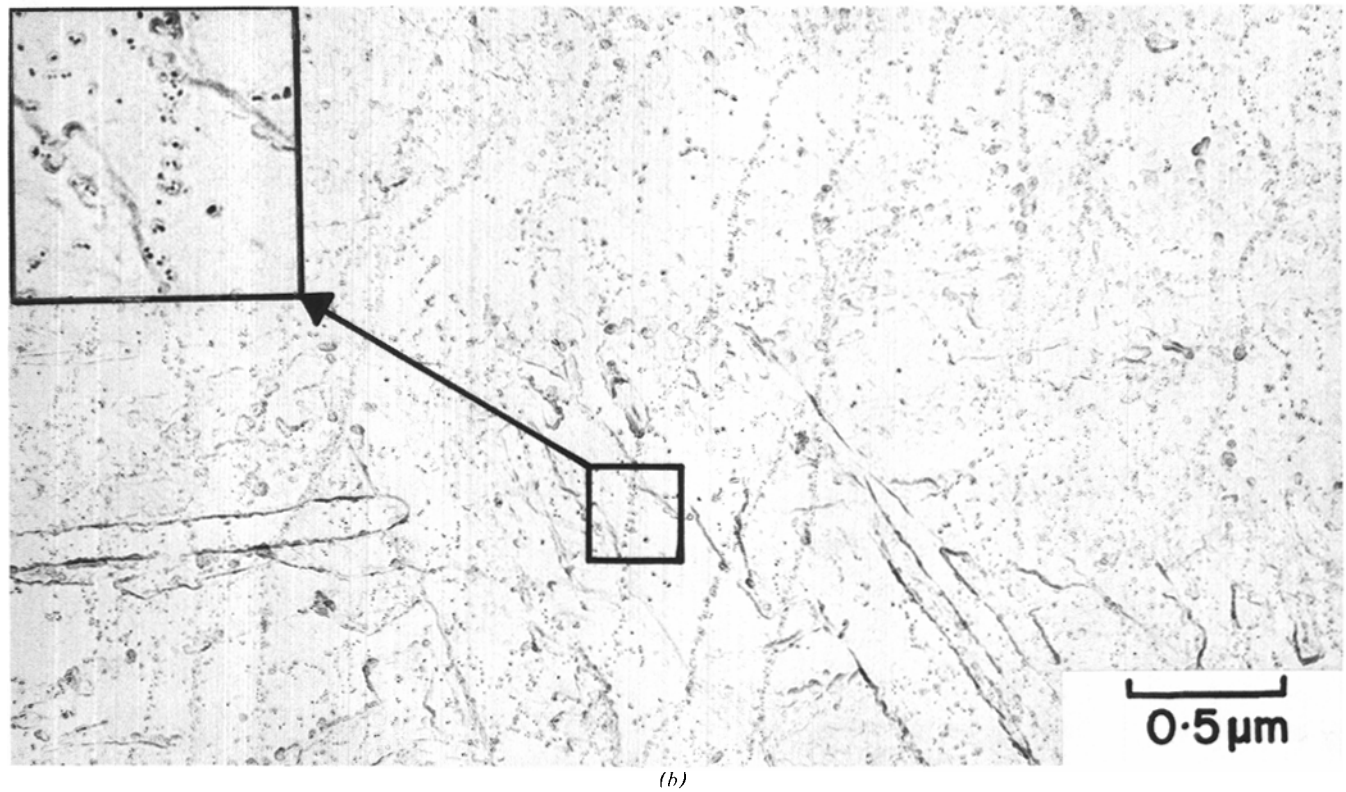

(b)

Fig. 11—Carbon extraction replicas of steel 3 hot rolled 50 pct at 950°C, illustrating (*a*) Nb(C, N) precipitation along a prior austenitic grain boundary after holding 10 s at 950°C, and (*b*) Nb(C, N) precipitation on prior austenitic substructure after holding 1,000 s at 900°C. In (*a*), some ferrite is also precipitated along a prior austenitic boundary, and is designated as "*F*" in comparison with the martensitic matrix "*M*". Inserts show fine Nb(C, N) particles at a further magnification of 2.5 times.

solution. On the other hand, the precipitation rate is greatly retarded if recrystallization precedes the precipitation.

Some of these effects are detailed in the following sections.

Precipitation Kinetics in the 0.03 Pct Nb Steels

The Nb(C,N) precipitation processes in steels 2 and 5 (0.03 pct Nb, solutionized at 1250°C) were found to be similar at 950°C, and so only steel 2 was evaluated at 850 and 900°C. The particle-size frequency distributions, and the K parameter for steel 2, are plotted in Figs. 12 and 13. The average particle diameter for each frequency distribution is indicated by arrows in Fig. 12. The precipitation reactions in these steels can be summarized as follows:

At 850°C, the grain-boundary precipitation occurs in about 100 s after rolling, and the matrix precipitation begins soon thereafter. Based on the K parameter, this matrix precipitation appears to be essentially complete after about 1,000 s. No significant coarsening of the matrix precipitates is observed even on prolonged holding at this temperature (Fig. 12). An average particle diam of about 3 to 4 nm is

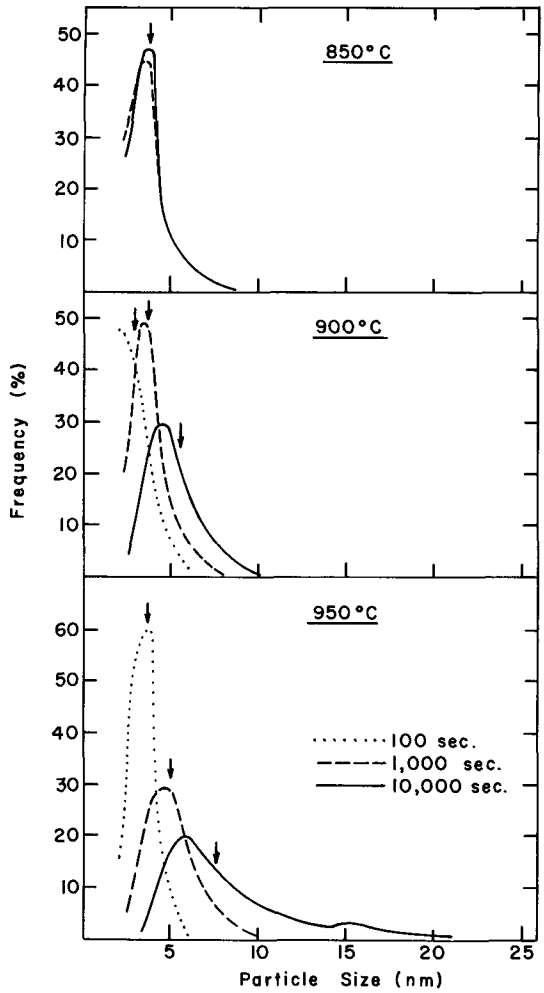

Fig. 12—Precipitate-size frequency distribution curves for steel 2 after solutionizing at 1250°C, hot rolling 50 pct at 950°C, and holding for various time/temperature combinations. Arrows indicate the average particle sizes for the respective distributions.

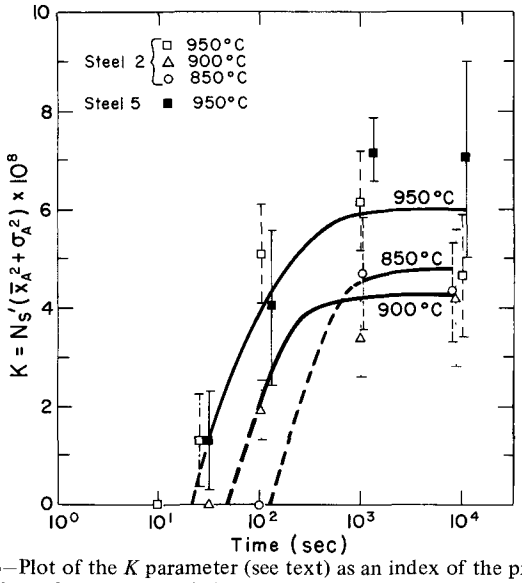

Fig. 13—Plot of the K parameter (see text) as an index of the precipitate volume fraction in steels 2 and 5, after solutionizing at 1250°C, hot rolling 50 pct at 950°C, and holding for various time/temperature combinations. Error bars represent ± 2σ from the average values.

retained, being possibly fine enough to provide some degree of precipitation strengthening in any subsequent transformation product.[41,42] At 900 and 950°C, similar patterns are followed, but with generally more rapid kinetics, although there is considerable scatter and overlap of the data. At these higher temperatures, precipitation starts between 10 and 100 s, and particle coarsening takes place to about 5 nm and 8 nm respectively in 10,000 s.

Markedly different precipitation kinetics are noted in steel 2 on solutionizing at 1100°C, and holding at 950°C after hot rolling. Although some grain-boundary precipitation is detected after 10 s, no significant matrix precipitation occurs, even within 10,000 s. For example, Fig. 14 compares the precipitate morphologies after 100 s at 950°C in steel 2, previously solutionized at 1100 and 1250°C. In the former instance (about 0.018 pct Nb in solution prior to hot rolling), no matrix precipitation is seen within 100 s at 950°C,* while virtually complete recrystallization of the austenite has taken place. In contrast, substantial matrix precipitation occurs within this holding period in the sample solutionized at 1250°C (about 0.031 pct Nb dissolved prior to rolling), and the austenite recrystallization reaches only 20 pct completion. This is a significant point: pronounced retardation of austenite recrystallization is found to be associated with Nb(C,N) matrix precipitation, while comparatively little retardation is observed without such precipitation. Apparently, with less than 0.02 pct Nb dissolved in the austenite prior to hot rolling, the ensuing Nb(C,N) precipitation kinetics are too slow for precipitation to occur prior to or during recrystallization, even though the austenite is supersaturated at this Nb concentration. Thus, the matrix precipitation, which eventually sets in, then takes place in recrystallized austenite, a process which is known to be relatively slow.[27]

*It should be noted that soaking steel 2 at 1100°C results in only a partial solution of the Nb(C,N) particles. The undissolved carbonitrides (see Fig. 2(*b*)) are also in Fig. 14(*a*) (40 to 100 nm in size), along with some finer precipitates (4 to 10 nm) formed after rolling.

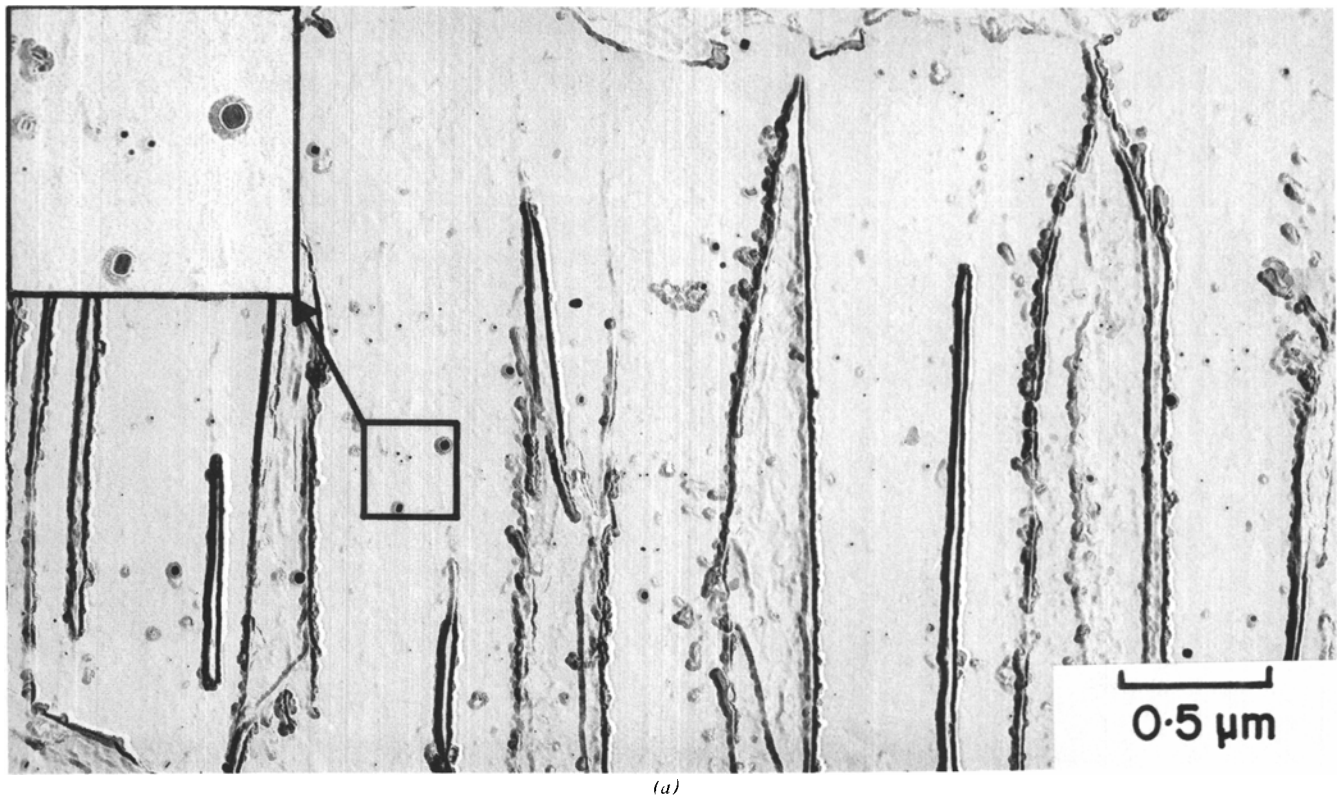

(a)

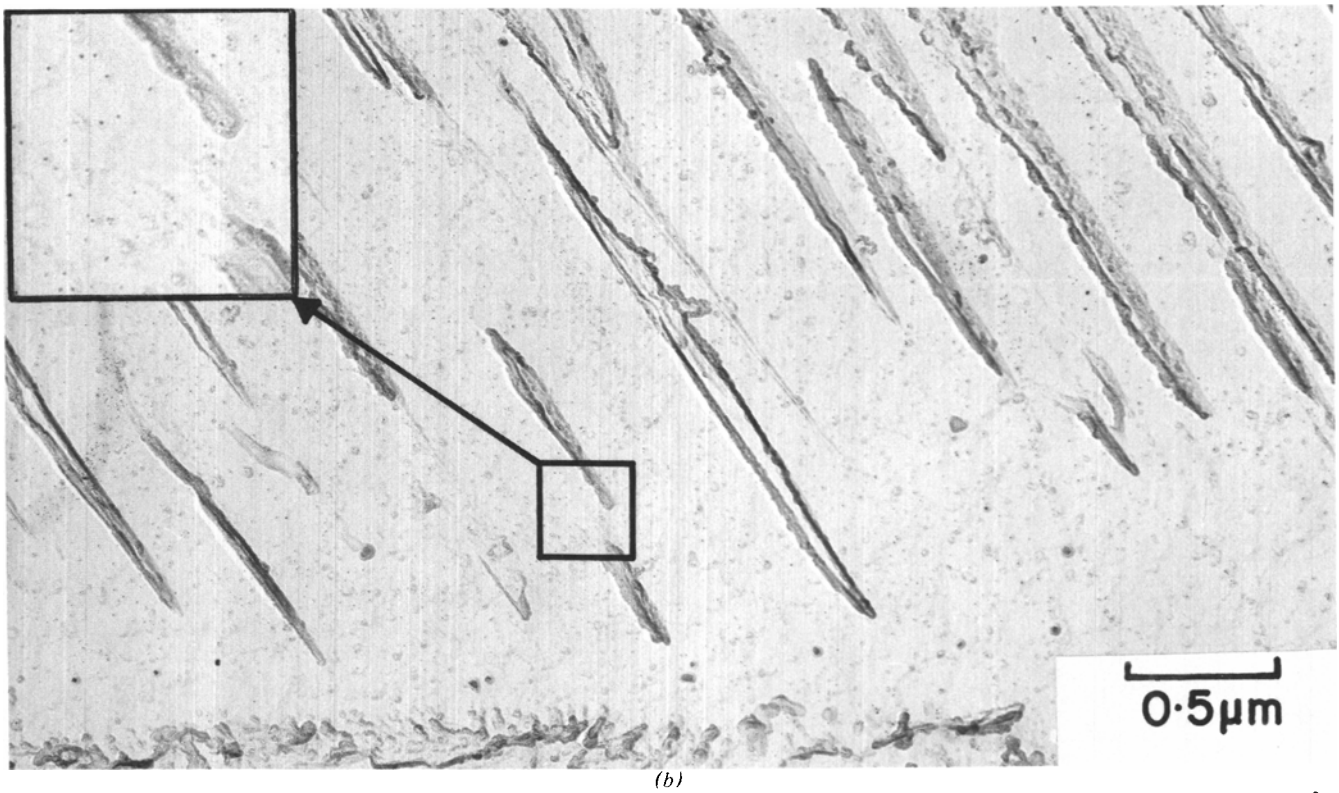

(b)

Fig. 14—Carbon extraction replicas illustrating effect of solutionizing temperature (level of dissolved niobium prior to hot rolling 50 pct at 950°C) on the Nb(C, N) precipitate morphology in steel 2 after holding at 950°C for 100 s. (*a*) Solutionized at 1100°C (~0.018 pct Nb in solution). (*b*) Solutionized at 1250°C (0.031 pct Nb in solution). Inserts show Nb(C, N) particles at a further magnification of 2.5 times.

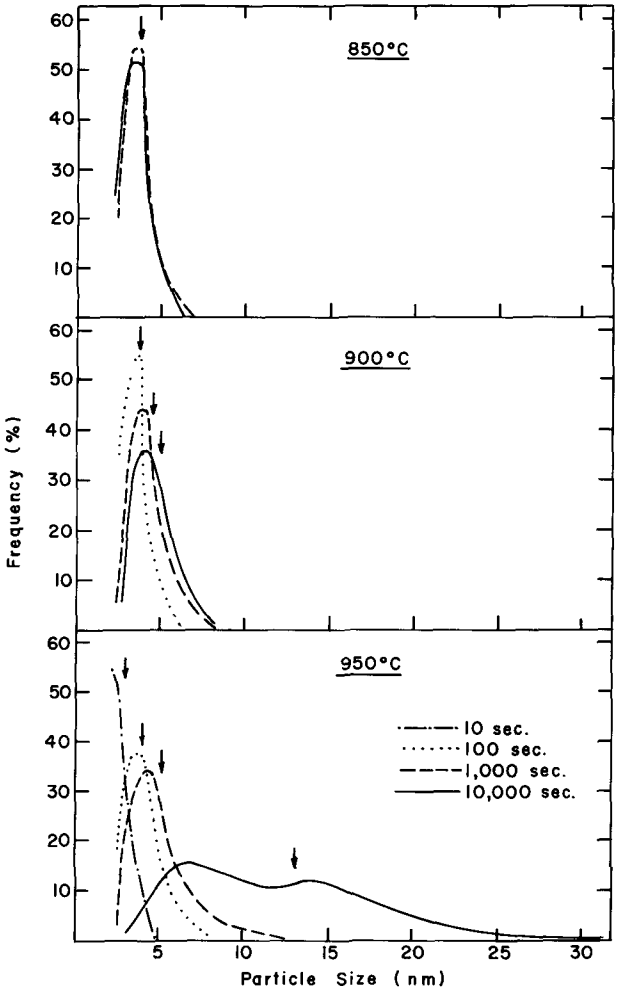

Fig. 15—Precipitate-size frequency distribution curves for steel 3 after solutionizing at 1250°C, hot rolling 50 pct at 950°C, and holding for various time-temperature combinations. Arrows indicate average particle sizes for the respective distributions.

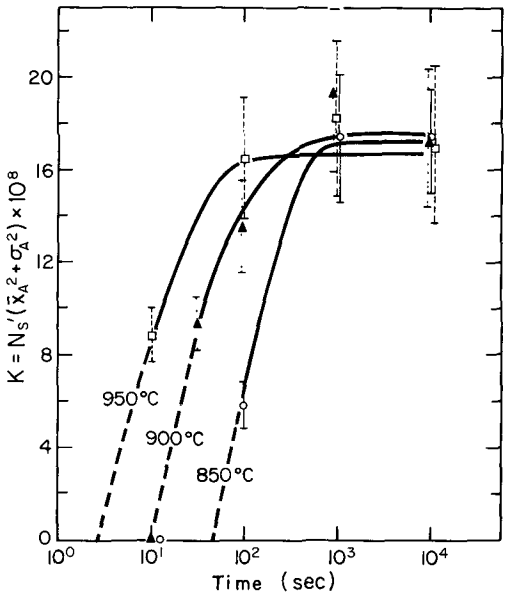

Fig. 16—Plot of the K parameter (see text) as an index of the precipitate volume fraction in steel 3 after solutionizing at 1250°C, hot rolling 50 pct at 950°C, and holding for various time/temperature combinations. Error bars represent ± 2σ from the average values.

Precipitation Kinetics in 0.095 Pct Nb and 0.21 Pct Nb Steels

Similar precipitation reactions at 950°C are observed in these higher-niobium steels, previously solutionized at 1250°C and hot rolled 50 pct at 950°C. The relevant precipitate-size distributions and K parameters for steel 3 (0.095 pct Nb) are presented in Figs. 15 and 16. Here, boundary precipitation is detected even on direct quenching off the rolls, and the Nb(C,N) matrix precipitation reaction is also faster compared to the 0.03 pct Nb steels. According to Fig. 16, the matrix precipitation is essentially complete between 100 and 1,000 s at 850 and 900°C, and within about 100 s at 950°C. Additionally, no appreciable particle coarsening occurs at 850°C (Fig. 15), while at 900°C the particles grow to an average size of about 4 to 5 nm in 10,000 s. At 950°C, substantial particle growth takes place, and a duplex particle size develops, seemingly due to preferential coarsening of precipitates on either subboundaries or dislocations. There is also some indication of a duplex particle size forming in steel 2 at this temperature (Fig. 12).

DISCUSSION

Recrystallization and Precipitation Reactions

Recrystallization/precipitation/temperature/time diagrams can now be constructed, as shown in Figs. 17 and 18 for steels 2 and 3. Here, the start-up of recrystallization (taken as 5 pct recrystallized) and 50 pct recrystallization are plotted, together with a broad band representing the approximate time period over which the Nb(C,N) matrix precipitation reaction takes place. A line denoting the entré of grain-boundary Nb(C,N) precipitation is also shown. In both steels, the Nb(C,N) precipitation precedes the start of recrystallization, although in steel 2 (Fig. 17) the two processes are tending to overlap at 950°C. When steel 2 is solutionized at 1100°C (diagram not shown), the austenite recrystallization is completed at 950°C prior to Nb(C,N) matrix precipitation. In this case, while there is some retardation of the recrystallization due to the dissolved Nb, this influence is minor in contrast to the pronounced retardation when Nb(C,N) matrix precipitation occurs prior to or during the early stages of austenite recrystallization (Fig. 8). Consequently, the conspicuous reduction in recrystallization growth rate when the solutionizing temperature is raised from 1100 to 1250°C (Fig. 9) must be attributed primarily to precipitate pinning rather than to solute drag.

In essence, then, there is a strong two-way interaction between austenite recrystallization and Nb(C,N) precipitation after hot rolling: (*a*) the precipitation reaction is accelerated by the substructure of the unrecrystallized austenite (strain-induced precipitation), and (*b*) the recrystallization process is retarded by the matrix precipitation of Nb(C,N) particles on austenitic subboundaries.

The following discussion relates to this recrystallization/precipitation interaction.

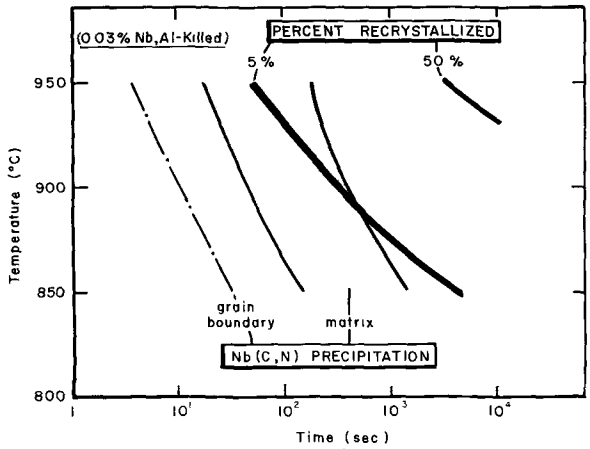

Fig. 17—Recrystallization/precipitation/temperature/time (RPTT) diagram for steel 2 after solutionizing at 1250°C and hot rolling 50 pct at 950°C.

Effect of Nb(C,N) Precipitates on Recrystallization Kinetics

The basic nucleation mechanism in recrystallization is still unresolved,[43] even in alloy systems which are much simpler than the microalloyed steels under investigation here. Therefore, one should not expect that the present results will discriminate between such viable mechanisms as subgrain growth[44,45] and strain-induced boundary migration.[46,47] On the other hand, recrystallization-front growth-rate measurements have been made here, and so we now direct attention to this part of the recrystallization reaction.

The driving force (F_R) for recrystallization-front migration can be estimated from the reduction in stored energy per unit volume traversed by the recrystallization front, assuming that dislocation annihilation is the operative process. On this basis, F_R is given by:[48]

$$F_R \simeq \left(\frac{\mu \mathbf{b}^2}{2}\right)(\Delta\rho),$$

where μ is the shear modulus ($\sim 7 \times 10^4$ MN/m^2 for steel), **b** is the Burgers vector ($\sim 2 \times 10^{-10}$ m), and $\Delta\rho$ is the change in dislocation density as the recrystallization front moves along (taken to be about 10^{16}/m^2 for the hot-rolled austenites involved). Then, F_R = 14 MN/m^2, in line with similar order-of-magnitude calculations.[49]

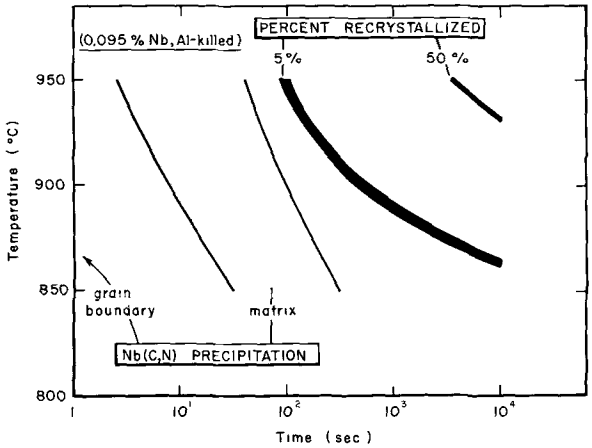

Fig. 18—Recrystallization/precipitation/temperature/time (RPTT) diagram for steel 3 after solutionizing at 1250°C and hot rolling 50 pct at 950°C.

Zener[33] originally pointed out that, in the presence of a second phase, grain-boundary migration may be inhibited because the second-phase particles replace part of the grain boundary, and this increment of grain-boundary area must be created if the boundary is to move away from the particles. More recently, Gladman[34] refined this idea, and derived a retarding force of $4r\gamma$ for each such spherical particle, where r is the particle radius, and γ is the interfacial energy per unit area of boundary. Thus, the retarding force (F_P) due to precipitated particles per unit area of boundary can be expressed as:

$$F_P = 4r\gamma N_S,$$

where N_S is the number of particles per unit area of boundary.

If $F_R < F_P$, the interfaces will be completely arrested, whereas if $F_R >> F_P$, the precipitates should not have any significant effect on the boundary migration. However, if $F_R > F_P$ and the magnitudes are comparable, the boundary may then move, but at some reduced overall velocity.

For a random dispersion of spherical particles (radius r and volume fraction f), the number of particles per unit volume is given by:

$$N_v = \frac{f}{4/3\pi r^3}$$

Assuming that all particles having centers within a distance r of the boundary will interact with the boundary, then $N_S = 2rN_v$, and

$$F_P = 4r\gamma(2rN_v) = \frac{6\gamma f}{\pi r}$$

Taking $\gamma \simeq 0.7$-0.8 J/m^2 in austenite,[50] for the finest average Nb(C,N) particles observed ($r \simeq 2$ nm), and for the maximum precipitate volume fractions measured in these steels ($4 \times 10^{-4} - 8.5 \times 10^{-4}$), $F_P \simeq 0.3$ to 0.6 MN/m^2 for the assumed random dispersion. This is a very small retarding force compared to the previously estimated $F_R \simeq 14$ MN/m^2.

A more realistic assumption for the precipitate distribution is that the particles lie on subboundaries in the hot-worked structure. If the average subboundary intercept is $\bar{l}$, the surface area per unit volume for such subboundaries is $2/\bar{l}$, and the number of particles per unit subboundary area is given by:

$$N_S \cdot b = \frac{N_v}{2/\bar{l}} = \frac{3f\bar{l}}{8\pi r^3}$$

The precipitate-retarding force corresponding to this case is:

$$F_P = 4r\gamma\left(\frac{3f\bar{l}}{8\pi r^3}\right) = \frac{3\gamma f\bar{l}}{2\pi r^2}$$

Using values already given for γ, r, and f, and for subboundaries of mean intercept $\bar{l} \simeq 0.5$ μm (from

observations made in this investigation), $F_P \simeq 20$ to 40 MN/m^2.

Thus, with the precipitated particles located preferentially on subboundaries in the hot-rolled austenite, the precipitate-pinning force appears to be of comparable magnitude to the driving force for recrystallization growth. Correspondingly, the observed Nb(C,N) particle sizes and volume fractions are evidently in the right range to retard recrystallization growth, with an increasing precipitate volume fraction producing slower growth rates, as indicated by Fig. 9. At the same time, the retarding force is expected to be quite sensitive to particle size, varying inversely as the square of the radius. This may account, at least in part, for the virtual completion of recrystallization at 950°C where the particles coarsen to an average diameter of about 8 nm in steel 2 and 13 nm in steel 3 after 10,000 s at temperature, in contrast to the lack of any significant recrystallization at 850°C where no particle coarsening is found even on prolonged holding.

Another point to be noted here is that, for the precipitate volume fractions encountered, *heterogeneous* precipitation on the scale of the substructure seems to be essential for retarding the recrystallization growth, and so plastic deformation plays an important role in the geometry as well as the kinetics of precipitation. This may explain the finding of LeBon *et al*[18] that Nb(C,N) precipitates existing *prior* to the plastic deformation have no appreciable retarding effect on recrystallization even though the particles may be in the 4 to 5 nm diam range.

Interaction Between Nb(C,N) Precipitation and Austenite Recrystallization

The interplay of precipitation and recrystallization phenomena have been studied previously in cold-work and annealed metals, for example by Kreye *et al* in Cu-Co alloys.[51]

For present purposes, the temperature dependence of recrystallization kinetics can be represented schematically by the recrystallization-start (R_s) and finish (R_f) curves in Fig. 19. If a retarding interaction comes into play, say between the recrystallization process and a precipitated phase, the time curves for the start and finish of recrystallization will be displaced to R_s^P and R_f^P in Fig. 19, designating both an increase in the incubation time for recrystallization

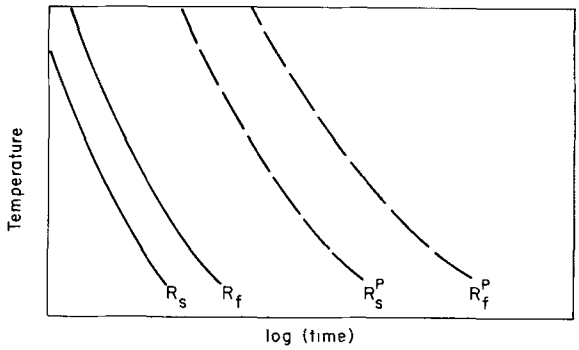

Fig. 19—Schematic recrystallization-start and finish curves (R_s and R_f) illustrating the retardation effect of precipitates on the recrystallization kinetics (R_s^P and R_f^P).

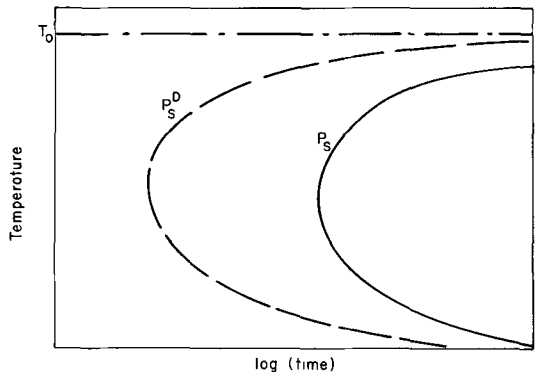

Fig. 20—Schematic precipitate-start *C*-curves illustrating the accelerating effect of plastic deformation on the precipitation kinetics (P_s *vs* P_s^D).

and a decrease in the subsequent recrystallization rate.

Analogously, the start of precipitation can be represented schematically by the *C*-curve (P_s) in Fig. 20, where T_0 is the equilibrium solubility temperature for the operative precipitation process (Nb(C, N) in austenite for the steels in this study). In the present context, T_0 usually corresponds to the solutionizing temperature or the solvus temperature, whichever is lower. The introduction of new and potent nucleation sites by plastic deformation has the effect of shifting the *C*-curve to shorter times (P_s^D) in Fig. 20.

The recrystallization/precipitation/temperature/time (RPTT) diagram in Fig. 21 is somewhat generalized, although it is based on experimental results obtained in this investigation. It highlights the mutual interaction of recrystallization (from Fig. 19) and precipitation (from Fig. 20). Obviously, above T_0, precipitation is thermodynamically impossible. Below T_0, however, three interaction regimes are possible. In regime 1, recrystallization is completed before precipitation starts (even with the potential accelerating effect of the prior plastic deformation) and thus no interaction is achieved. Accordingly, precipitation eventually takes place in the recrystallized austenite along the P_s curve. The recrystallization process, preceding any such precipitation in this case, is defined by the R_s and R_f curves.

In regime 2, although the initiation of recrystalliza-

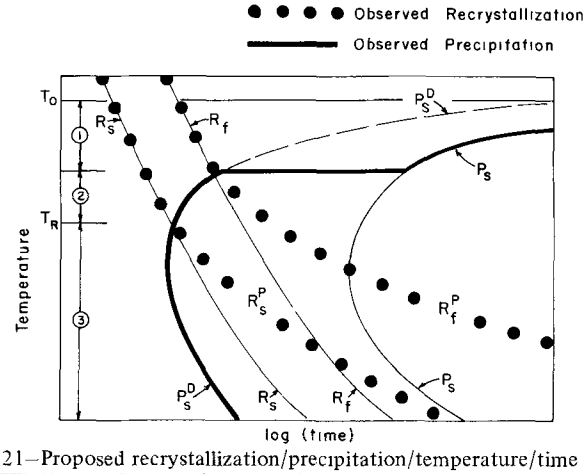

Fig. 21—Proposed recrystallization/precipitation/temperature/time (RPTT) diagram for a steel characterized by the precipitate solubility temperature T_0. T_R is the temperature below which there is maximum interaction between the recrystallization and precipitation processes.

tion precedes precipitation, the latter reaction sets in before recrystallization is complete, and so the end of recrystallization is delayed. Hence, in this regime, precipitation starts along the P_s^D curve, while recrystallization starts along the R_s curve, but ends along R_f^P curve. In regime 3, precipitation takes place before recrystallization (*i.e.*, along the P_s^D curve), and now both the start and finish of recrystallization are delayed (to the R_s^P and R_f^P curves).

Over the three temperature regimes below T_0, the start and finish of the recrystallization reaction are designated by the solid circles in Fig. 21. Concurrently, the precipitation reaction shifts from the P_s curve in regime 1 to the P_s^D curve in regimes 2 and 3, as indicated by the heavy lines. Regime 3 behavior is desirable from the standpoint of maximizing the precipitation/recrystallization interaction and, therefore, retarding recrystallization of the austenite.

In the present experiments, regime 3 behavior is observed in steels 2 and 3 solutionized at 1250°C (Figs. 17 and 18) at all the post-rolling temperatures studied, although a transition to regime 2 seems near in steel 2 at 950°C. However, steel 2 solutionized at 1100°C exhibits regime 1 behavior at 950°C. The precipitation/recrystallization interactions and, in fact, the actual temperature ranges over which the various regimes are operative are sensitive to the degree of supersaturation or to the temperature interval between T_0 and the post-roll holding temperature. Sufficient supercooling is necessary for any interaction to occur. But, if T_0 is too low, regimes 3 and even 2 may be cut off by austenite decomposition into ferritic transformation products. It is suggested that a critical degree of supersaturation may have to be exceeded, given the hot-rolling conditions adopted here, in order that the strain-induced precipitation will occur rapidly enough to "head off" the austenite recrystallization, as in regime 3. For example, we have shown that 0.03 pct Nb in solution (plus 0.1 pct C and 0.01 pct N) is sufficient for strain-induced precipitation to ensue and retard recrystallization of the hot-rolled austenite at 950°C, whereas 0.02 pct Nb (plus 0.1 pct C and 0.01 pct N) is not sufficient. These two compositions correspond to supersaturation ratios of 7.5 and 5 at 950°C respectively, based on the Irvine *et al* solubility equation,[2] and so the aforementioned critical supersaturation seems to fall between these limits for the particular conditions under study.

CONCLUSIONS

The major findings of this investigation on Nb-microalloyed steels can be summarized as follows:

1. Niobium in supersaturated solution prior to hot deformation sets the stage for retardation of austenite recrystallization; the degree of this retardation increases with the concentration of dissolved niobium, and with decreasing holding temperature. Although the dissolved niobium *per se* may have some effect on the recrystallization kinetics, the major retardation is due to Nb(C,N) precipitation, which results in an increase in the incubation time for austenite recrystallization as well as a much slower recrystallization growth rate.

2. Manganese variations in the range of 1.3 to 2.0 pct Mn appear to have no significant influence on the austenite-recrystallization or Nb(C,N)-precipitation kinetics in a 0.03 pct Nb steel.

3. Strain-induced Nb(C,N) precipitation from hot-rolled austenite occurs in two stages: (a) initial precipitation at prior austenitic grain boundaries and deformation bands, and (b) general matrix precipitation on the substructure of the unrecrystallized austenite. If austenite recrystallization precedes the precipitation, the latter then sets in relatively slowly in the recrystallized matrix.

4. The fine Nb(C,N) matrix precipitates do not coarsen on prolonged holding at 850°C. However, particle growth takes place at higher temperatures, and prolonged holding at 950°C leads to a duplex precipitate-size distribution.

5. The observed Nb(C,N) precipitate morphologies are shown to be capable of providing recrystallization-growth retarding forces comparable in magnitude to the driving force for recrystallization. As a result, the effects of particle size, volume fraction, and degree of supersaturation prior to the hot working can be rationalized.

6. The Nb(C,N)-precipitation and austenite-recrystallization reactions are found to be coupled phenomena, with the precipitation being accelerated (strain-induced) by the substructure of the hot-worked (unrecrystallized) austenite, and the recrystallization then being retarded by the pinning effect of the precipitated particles. The degree of supersaturation with respect to Nb(C,N) is believed to be a critical factor in determining whether or not an effective recrystallization/precipitation interaction will take place at a particular temperature.

ACKNOWLEDGMENTS

The authors are indebted to the Bethlehem Steel Corporation for supplying the experimental steels used in this investigation, and for financial support of one of the authors (SSH) during his graduate studies at MIT. We are also grateful to S. A. Kulin, H. Tushman, and P. Neshe of ManLabs, Inc. for access to their rolling facilities and for their invaluable assistance during the course of the hot-rolling experiments. Thanks are likewise due to A. J. Gregor, M. A. Meyer, and N. S. Naugle for their help in many ways leading to the eventual preparation of this paper. The results reported here are taken from a thesis submitted by S. S. Hansen for the Doctor of Science degree at the Massachusetts Institute of Technology in February 1978.

REFERENCES

1. W. E. Duckworth, R. Phillips, and J. A. Chapman: *J. Iron Steel Inst.*, 1965, vol. 203, p. 1108.
2. K. J. Irvine, F. B. Pickering, and T. Gladman. *J. Iron and Steel Inst.*, 1967, vol. 205, p. 161.
3. F. B. Pickering: *Microalloying 75, Proceedings*, p. 9, Union Carbide Corporation, New York, 1977.
4. T. Gladman, D. Dulieu, and I. D. McIvor: *Microalloying 75, Proceedings*, p. 32, Union Carbide Corporation, New York, 1977.
5. L. Meyer, F. Heisterkamp, and W. Mueschenborn: *Microalloying 75, Proceedings*, p. 153, Union Carbide Corporation, New York, 1977.
6. J. D. Baird and R. R. Preston: *Processing and Properties of Low Carbon Steel,*

p. 1, The Metallurgical Society of AIME, New York, 1973.
7. M. Cohen and S. S. Hansen: *MICON '78· Optimization of Processing, Properties and Service Performance Through Microstructural Control,* H. Abrams, G. N. Manian, D. A. Nail, and H. D. Solomon, eds., p. 34, ASTM, Philadelphia, PA, 1979.
8. K. J. Irvine, T. Gladman, J. Orr, and F. B. Pickering: *J. Iron Steel Inst.,* 1970, vol. 208, p. 717.
9. R. A. P. Djaic and J. J. Jonas: *J. Iron Steel Inst.,* 1972, vol. 210, p. 256.
10. R. A. Petkovic, M. J. Luton, and J. J. Jonas: *Can. Met. Quart.,* 1975, vol. 14, p. 137.
11. R. A. Petkovic, M. J. Luton, and J. J. Jonas *The Hot Deformation of Austenite,* p. 68, The Metallurgical Society of AIME, New York, 1977.
12. M. J. Stewart: *The Hot Deformation of Austenite,* p. 233, The Metallurgical Society of AIME, New York, 1977.
13. L. J. Cuddy: *The Hot Deformation of Austenite,* p. 169, The Metallurgical Society of AIME, New York, 1977.
14. J. N. Cordea and R. E. Hook· *Met. Trans.,* 1970, vol. 1, p. 111.
15. T. L. Capaletti, L. A. Jackson, and W. J. Childs: *Met. Trans.,* 1972, vol. 3, p. 789.
16. H. Weiss, A. Gittins, G. G. Brown, and W. J. McG. Tegart· *J. Iron Steel Inst.,* 1973, vol. 211, p. 703.
17. A. LeBon, J. Rofes-Vernis, and C. Rossard: *Mem. Sci. Rev. Met.,* 1973, vol. 70, p. 577.
18. A. LeBon, J. Rofes-Vernis, and C. Rossard: *Met. Sci.,* 1975, vol. 9, p. 36.
19. K. J. Irvine, T. Gladman, J. Orr, and F. B. Pickering *J. Iron Steel Inst.,* 1970, vol 208, p. 717.
20. J. D. Jones and A. B. Rothwell. *Iron Steel Inst., Publication No. 108,* 1968, p. 78.
21. R. Preistner, C. C. Early, and J. H. Rendall: *J. Iron Steel Inst.,* 1968, vol. 206, p. 1252.
22. I. Kosazu, T. Shimuzu, and H. Kubota *Trans. Iron Steel Inst. Jpn,* 1971, vol. 11, p. 367.
23. B. L. Phillipo and F. A. A. Crane: *J. Iron Steel Inst.,* 1973, vol. 211, p. 653.
24. H. Sekine and T. Maruyama: *Trans. Iron Steel Inst. Jpn,* 1976, vol. 16, p. 427.
25. T. M. Hoogendoorn and M. J. Spanraft *Microalloying 75, Proceedings,* p. 75, Union Carbide Corporation, New York, 1977.
26. A. T. Davenport, R. E. Miner, and R. A. Kot: *The Hot Deformation of Austenite,* p. 186, The Metallurgical Society of AIME, New York, 1977.
27. H. Watanabe, Y. E. Smith, and R. D. Pehlke: *The Hot Deformation of Austenite,* p. 140, The Metallurgical Society of AIME, New York, 1977.
28. I. Weiss and J. J. Jonas: *Met. Trans. A,* 1979, vol. 10A, p. 831.
29. I. Weiss and J. J. Jonas: *Met. Sci.,* 1979, vol. 13, p. 238.
30. H. Nordberg and B. Aronsson: *J. Iron Steel Inst.,* 1968, vol. 206, p. 1263.
31. G. E. Dieter, Jr.: *Mechanical Metallurgy,* 1st edition, p. 509, McGraw-Hill Book Co., New York, 1961.
32. M. F. Ashby and R. Ebeling: *Trans. TMS-AIME,* 1966, vol. 236, p. 1396.
33. C. Zener (1949)—Private communication to C. S. Smith: *Trans. AIME,* 1949, vol. 175, p. 15.
34. T. Gladman· *Proc. Roy. Soc.,* 1966, vol. A294, p. 298.
35. A. T. English and W. A. Backofen: *Trans. TMS-AIME,* 1964, vol. 230, p. 396.
36. C. Wells: *Atom Movements,* p. 30, American Society for Metals Publication, Metals Park, Ohio, 1951.
37. T. Gladman, I. D. McIvor, and F. B. Pickering. *J. Iron Steel Inst.,* 1971, vol. 209, p. 380.
38. J. W. Cahn. *Acta Met.,* 1956, vol. 4, p. 449.
39. J. W. Cahn and W. C. Hagel· *Acta Met.,* 1963, vol. 11, p. 561.
40. G. R. Speich and R. M. Fisher: *Recrystallization, Grain Growth and Textures,* p. 563, ASM Publication, Metals Park, Ohio, 1966.
41. M. F. Ashby: *Oxide Dispersion Strengthening,* p. 143, The Metallurgical Society of AIME, New York, 1958.
42. T. Gladman, B. Holmes, and I. D. McIvor: *The Effects of Second Phase Particles on the Mechanical Properties of Steel,* p. 68, The Iron and Steel Institute, London, England, 1971.
43. R. W. Cahn. *Recrystallization, Grain Growth and Textures,* p. 99, ASM Publication, Metals Park, Ohio, 1966.
44. E. Orowan: *Dislocations in Metals,* p. 181, AIME Publication, New York, 1954.
45. H. Hu: *Recovery and Recrystallization of Metals,* p. 311, Interscience Publishers, New York, 1963.
46. P. A. Beck and P. R. Sperry: *J. Appl. Phys.,* 1950, vol. 21, p. 150.
47. J. E. Bailey and P. B. Hirsch: *Proc. Roy. Soc.,* 1962, vol. A267, p. 11.
48. U. F. Kocks, A. S. Argon, and M. F. Ashby: *Progress in Materials Science,* vol. 19, Pergamon Press, New York, 1976.
49. H. Gleiter and B. Chalmers: *Progress in Materials Science,* vol. 16, Pergamon Press, New York, 1972.
50. L. E. Murr *Interfacial Phenomena in Metals and Alloys,* Addison-Wesley, Reading, MA, 1975.
51. H. Kreye and E. Hornbogen: *J. Mater. Sci.,* 1970, vol. 5, p. 89.